Antisites in III-V semiconductors: Density functional theory calculations

Chroneos, A. , Tahini, H.A. , Schwingenschlögl, U. and Grimes, R.W.

Original citation:
Chroneos, A. , Tahini, H.A. , Schwingenschlögl, U. and Grimes, R.W. (2014) Antisites in III-V semiconductors: Density functional theory calculations. Journal of Applied Physics, volume 116 (Article number 023505). DOI: 10.1063/1.4887135

http://dx.doi.org/10.1063/1.4887135

American Institute of Physics

Antisites in III-V semiconductors: Density functional theory calculations

A. Chroneos,[1,*] H. A. Tahini,[2,3] U. Schwingenschlögl,[3,§] and R. W. Grimes[2,‡]

[1]*Engineering and Innovation, The Open University, Milton Keynes MK7 6AA, UK*
[2]*Department of Materials, Imperial College London, London SW7 2AZ, UK*
[3]*PSE Division, KAUST, Thuwal 23955-6900, Kingdom of Saudi Arabia*

Abstract

Density functional based simulation, corrected for finite size effects, is used to investigate systematically the formation of antisite defects in III-V semiconductors (III = Al, Ga and In and V = P, As and Sb). Different charge states are modelled, as a function of the Fermi level and under different growth conditions. The formation energies of group III antisites (III_V^q) decrease with increasing covalent radius of the group V atom though not group III radius, whereas group V antisites (V_{III}^q) show a consistent decrease in formation energies with increase in group III and group V covalent radii. In general, III_V^q defects dominate under III-rich conditions and V_{III}^q under V-rich conditions. Comparison with equivalent vacancy formation energy simulations shows that while antisite concentrations are always dominant under stoichiometric conditions, modest variation in growth or doping conditions can lead to a significantly higher concentration of vacancies.

* A. Chroneos: alex.chroneos@open.ac.uk; §U. Schwingenschlögl: udo.schwingenschlogl@kaust.edu.sa;‡ R. W. Grimes: r.grimes@imperial.ac.uk

I. INTRODUCTION

The search for silicon alternate materials has led to a regeneration of interest in materials such as germanium and III-V semiconductors. The latter are expected to play a crucial role as proposed by the International Technology Roadmap for semiconductors.[1] This is due to their advantageous material properties that can include high electron mobility, narrow direct band gap and lattice matching with ternary or quaternary III-V compounds.[2-7] These properties mean that III-V materials are important for nanoelectronic devices (for example GaAs or InAs)[2], for lasers (direct band gap materials such as InP)[8] and radiation detectors (indirect band gap materials such as AlAs or AlSb).

Theoretical studies are used to provide fundamental insights into the defect processes of group III-V semiconductors.[5-7] For the efficient miniaturization of electronic devices, it is important to understand the defects formed during the growth processes and their interaction with dopants. Antisites in III-V semiconductors are of fundamental and technological importance as they have a key role in diffusion properties.[9-12] For example, their interaction with vacancies has been studied to explain issues such as the asymmetric diffusion properties of the group III and V elements in GaAs and GaSb (see Ref. 12 and references therein). The electron or hole trapping characteristics of antisite defects may also be important in limiting device efficiency.

The aim of this study is to provide a consistent and systematic investigation of antisites in binary III-V semiconductors. The manuscript is organized as follows: in Sec. II, we discuss the methodology in terms of the computational parameters employed and the charge correction scheme used. The results of each III-V semiconductor are presented in Sec. III. Finally, we consider trends and draw conclusions, partly by comparing with equivalent vacancy formation energies.

II. COMPUTATIONAL METHODOLOGY

Density functional theory as implemented in the Vienna *Ab initio* Simulation Package[13] is

used to calculate total energies. The generalised gradient approximation with the Perdew, Burke and Ernzerhof formalism[14] was used to describe the electronic exchange and correlation. Pseudopotentials were generated using the projector augmented-wave method[15] and used together with a plane-wave basis with a cut-off energy of 400 eV. Three and five electrons were used to describe valence electrons in III and V atoms respectively. As was mentioned in our previous work[16], the use of more electrons leads only to a small change in the formation energies. The Brillouin zone was sampled using the Monkhorst-Pack scheme[17] using a mesh of 2 *x* 2 *x* 2 for the 216 supercell. Convergence criteria for energies and forces were 10^{-5} eV and 10^{-3} eV/Å respectively. All the calculations were spin-polarised and the defect containing supercells were simulated under constant volume conditions. Formation energies, E^f, were calculated based on the approach of Zhang and Northrup[18] as described by El-Mellouhi and Mousseau[19]:

$$E^f = E_{tot}(D,q) - E_{tot}(perfect) + \sum_\alpha n_\alpha \mu_\alpha + q\mu_e \mp \tfrac{1}{2}\Delta_\mu + E_{corr} \quad (1)$$

where $E_{tot}(D, q)$ is the energy of the defective cell with a charge q and E_{tot}(perfect) is the energy of the perfect cell. n_α is the number of atoms added or removed multiplied by their corresponding chemical potentials, μ_α. μ_e is the Fermi level referenced to the top of the valence band. $\Delta\mu$ is the chemical potential difference with the upper sign corresponding to group V vacancies and the lower sign to group III vacancies. The upper and lower bounds of $\Delta\mu$ are given by $-\Delta H \leq \Delta\mu \leq +\Delta H$, where ΔH is the heat of formation of a compound given by:

$$\Delta H_{III-V} = \mu_{III-V}^{bulk} - \mu_{III}^{bulk} - \mu_V^{bulk} \quad (2)$$

Finally, E_{corr} is a formation energy correction term. This accounts for the charged defect-defect interactions and was modelled using the recent scheme by Freysoldt *et al.*[20,21] Due to the well-known DFT band gap underestimation the experimental band gaps were used in Figs. 1-3

III. RESULTS

A. Aluminium-V Compounds

Formation energies for III-V semiconductors are presented in Fig 1 for Al-Vs, Fig 2 for Ga-Vs and Fig 3 for In-Vs.

1. Aluminium Phosphide

Fig 1a indicates that under stoichiometric conditions P_{Al}^{q} is easier to form than Al_{P}^{q} for all values of the Fermi energy, although the preferred charge state of the P_{Al}^{q} defect varies from +2 to -2 as the Fermi level changes from the valence band maximum (VBM) to the conduction band minimum (CBM). Under *p*-doping, P_{Al}^{q} forms in the +2 charge state with a formation energy of 1.41 eV at the VBM. This charge state persists up to a Fermi level of 0.61 eV when a transition to +1 charge state occurs. P_{Al}^{0} occurs from near the middle of the band gap and extends up to the *n*-doping region, by which point the formation energy is 3.01 eV, before making transitions to -1 and -2 at μ_e = 1.95 eV and μ_e = 2.12 eV respectively. In comparison, Al_{P}^{q} forms in the +1 charge state under p-doping conditions but with a higher formation energy than P_{Al}^{q} (2.47 eV higher than P_{Al}^{+2} at the VBM). At μ_e = 0.59 eV P_{Al}^{q} transitions to the neutral charge state and then -1 at μ_e = 1.11 eV and finally -2 at μ_e = 1.66 eV. At the CBM the difference in formation energies of Al_{P}^{-2} and P_{Al}^{-2} is only 0.2 eV.

Under Al-rich conditions Al_{P}^{q} becomes the dominant defect for the entire range of the band gap. P_{Al}^{+2} is about 0.2 eV higher than Al_{P}^{+1} at the VBM. However, due to their charges, the formation energies of the two antisites diverge and the difference becomes more than 1 eV from the middle of the band gap up to the CBM where the difference is 2.45 eV.

Since P_{Al}^{q} is favoured under stoichiometric conditions this should be maintained into the P-rich regime as is indicated in Fig 1a. Indeed, at the VBM P_{Al}^{+2} has a low formation energy of

0.09 eV whereas Al_P^{+1} requires 5.20 eV to form, rendering its concentration extremely low. Even as the Fermi level is shifted towards the CBM the Al_P^{-2} formation energy, 3.54 eV, is still high.

2. Aluminium Arsenide

Under all composition conditions, As_{Al}^{q} forms as As_{Al}^{+1} close to the VBM, As_{Al}^{0} at intermediate values of the Fermi level and As_{Al}^{-1} close to the CBM. Al_{As}^{q} defects are similar except that close to the CBM the lowest energy state is Al_{As}^{-2}. Thus, Al_{As}^{q} exhibits charge states as a function of Fermi level similar to Al_P^q in AlP whereas As_{Al}^{q} does not quite transition to the -2 charge state close to the CBM whereas P_{Al}^{q} does.

For stoichiometric conditions, As_{Al}^{q}, charge states, exhibit lower formation energies than the corresponding Al_{As}^{q} defects, except very close to the CBM, where the formation energy of the -2 charge state of Al_{As}^{q} is essentially the same as that for As_{Al}^{-1} . Thus, under *p*-doping and at the middle of the band gap Al_{As}^{q} is unlikely to form due to its large formation energy compared to As_{Al}^{q}. This starts to change rapidly as a transition *c*($-/=$) occurs at 1.68 eV which causes its formation energy to drop enough for it to form under extreme *n*-doping conditions.

Under Al-rich conditions Al_{As}^{q} is dominant for the entire band gap with the separation in formation energies between Al_{As}^{q} and As_{Al}^{q} reaching its maximum of 2.1 eV at the CBM. Moving to As-rich conditions favours As_{Al}^{q} for the whole Fermi level region, with large formation energy differences between the two antisites (3.76 eV and 1.90 eV at the VBM and CBM respectively) so that Al_{As}^{q} defects will exhibit very low concentrations.

3. Aluminium Antimonide

AlSb exhibits defect energies that are generally smaller than those in AlP or AlAs resulting in the maximum of the y-axis scale of Fig 1c being half that of Figs 1a and 1b. That is, the less favourable antisite defect for AlSb is not nearly so unfavourable as those in AlP or AlAs

for all Fermi levels and growth conditions. Conversely, the distribution of charge states as a function of Fermi level are very similar for all three materials

Considering now stoichiometric growth conditions, the defect with the lowest formation energy is Sb_{Al}^{+1} under p-doping conditions, which undergoes a transition to Sb_{Al}^{0} at μ_e = 0.41 eV. From the middle of the band gap and into the *n*-doping regime, the lowest energy defect is Al_{Sb}^{-2}. This is quite different to AlP and AlAs where P_{Al}^{q} and As_{Al}^{q} defects are of lowest formation energy for almost all Fermi energy values.

Under Al-rich conditions Al_{Sb}^{q} defects are more favourable compared to Sb_{Al}^{q} allowing the Al antisites a wider range of stability, which extends from μ_e = 0.52 eV to the CBM. Nevertheless, below this Fermi level Sb_{Al}^{+1} dominates under *p*-doping conditions and also marginally in the neutral charge state (see the left panel of Fig 1c). Under Sb-rich conditions the preferences are reversed. Now, Sb_{Al}^{q} exists over a wider Fermi level range, extending from the VBM for which it has a formation energy of 0.90 eV up to μ_e = 1.23 eV where Al_{Sb}^{q} becomes dominant and with decreasing energy as the level of *n*-doping is increased, until its lowest formation energy of 0.45 eV is achieved at the CBM.

B. Gallium-V Compounds

Broadly, for all three Ga-V materials, across growth conditions and Fermi levels, the energies and charge preferences of defects involving P, As or Sb on Ga sites are very similar to those of P, As or Sb on Al sites in the Al-V materials. Conversely, antisite defects, where Ga occupies P, As or Sb sites in Ga-V materials, are roughly 1 eV lower in energy than corresponding defects in Al-V materials. This leads to differences in cross-over between the most favourable antisite species so that Ga atoms occupying P, As or Sb sites often becoming most stable at lower Fermi levels. Also, for GaAs and GaSb systems there have been previous modelling studies with which we will compare.

1. Gallium Phosphide

Under stoichiometric conditions, Ga_P^q and P_{Ga}^q exhibit similar formation energies under *p*-doping conditions though P_{Ga}^q is the favourable defect. As the P antisite is in the +2 charge state, its formation energy increases with increasing Fermi level and even after a transition to the +1 charge, albeit at a slower rate. This reduces the difference in formation energies compared with the Ga antisite, which only exists very briefly in the +1 charge state close to the VBM but then acts as a shallow acceptor with a transition at μ_e = 0.07 eV to the neutral charge state making a further transition to the -1 charge state at μ_e = 1.00 eV. Thus, beyond a Fermi level of 0.59 eV the lowest energy species becomes Ga_P^q which becomes much more preferable as it accepts an additional electron towards *n*-doping conditions.

Under Ga-rich conditions, Ga antisites are clearly the favoured species for the entire band gap with P_{Ga}^q much higher in energy, reducing their concentration considerably in comparison to Ga antisite defects. Under p-rich growth conditions, P_{Ga}^q are stable for a wider range of Fermi level only superseded by Ga_P^{-2} at μ_e = 1.66 eV.

2. Gallium Arsenide

In GaAs, under stoichiometric conditions, the two antisites, Ga_{As}^q and As_{Ga}^q, exhibit very similar formation energies around Fermi levels in the middle of the band gap. As_{Ga}^q is the more stable in the +1 charge state and then neutral charge states under *p*-doping up to a Fermi level of 0.52 eV after which Ga_{As}^q becomes more stable in -1 and then -2 and finally -3 charge states. At the middle of the band gap As_{Ga}^0 has a formation energy of 1.95 eV, which is similar to the value of 2.29 eV reported by Pöykkö *et al.*[22] for the same defect under the same conditions.

Under Ga-rich conditions, Ga_{As}^q dominates for the entirety of the band gap. Ga_{As}^0 has a formation energy of 1.50 eV which is comparable to the value 1.70 eV found by Northrup and

Zhang[23]. Conversely As-rich growth conditions favour As_{Ga}^{q} for most of the band gap. Only under extreme *n*-doping conditions does Ga_{As}^{-3} eventually exhibit nearly the same formation energy as As_{Ga}^{-2}. In the middle of the band gap the formation energies for As_{Ga}^{q} and Ga_{As}^{q} are 1.23 eV and 2.92 eV respectively, which are in very good agreement with 1.27 eV and 3.20 eV, the results of Schultz and von Lilienfeld[24] under the same As-rich conditions.

3. Gallium Antimonide

Under stoichiometric conditions Ga_{Sb}^{q} is stable in the neutral charge state at the VBM with a formation energy of 1.09 eV, in good agreement with Hakala *et al.*[25] who calculated a formation energy of Ga_{Sb}^{0} 1.13 eV. Under the same conditions, the formation energy of Sb_{Ga}^{+1} is 0.36 eV higher. Ga_{Sb}^{0} is only stable over a very narrow Fermi energy range before accepting an electron forming Ga_{Sb}^{-1} at a shallow acceptor level,$c(0/-)$ = 0.04 eV. This Fermi energy value is identical to that calculated by Hakala *et al.*[25] The second transition occurs at $c(-/=)$ = 0.27 eV, again in good agreement with the value of 0.26 eV calculated by Hakala *et al.*[25] With increasing Fermi energy the formation energy of Ga_{Sb}^{q}falls compared to that of Sb_{Ga}^{q}, which means that Ga_{Sb}^{q} is dominant across the entire band gap (see Fig 2c).

Under Ga-rich conditions, the stability of Ga_{Sb}^{q} is further enhanced so again the concentration of Ga_{Sb}^{q} is much higher than that of Sb_{Ga}^{q}. However, for Sb-rich conditions, Sb_{Ga}^{q} in the +1 charge state under *p*-doping conditions is the most stable defect until at μ_e = 0.19 eV, when now in the neutral state, it becomes less stable than Ga_{Sb}^{-1}.

C. Indium-V Compounds

1. Indium Phosphide

The charge states exhibited and dominance of In_{P}^{q} or P_{In}^{q} defects is very similar to equivalent species in AlP and to a lesser extent in GaP – except that the formation energies are

generally a little lower. Under stoichiometric conditions, from the VBM up to μ_e = 1.14 eV P_{In}^{q} is the low energy defect with charge states +2, +1 and then neutral. Thereafter In_P^{q} in -1 and then -2 is dominant. At a Fermi energy in the centre of the band gap the calculated formation energy of P_{In}^{0} is 2.20 eV, exactly the same as that reported by Mishra *et al.*[27] and in very good agreement with the value of 2.28 eV calculated by Castleton and Mirbt[26]. A similar level of agreement is found for In_P^{0} where the formation energy of 2.67 eV is within 0.02 eV and 0.01 eV of the values reported in Refs. 26 and 27 respectively.

Under In-rich conditions, the formation energies of In_P^{+1} and P_{In}^{+2} are only separated by 0.08 eV at the VBM. However, this difference grows rapidly as P_{In}^{+1} rises in energy with increasing Fermi level whereas the initially neutral In_P^{q} traps an electron to form -1 and then -2 charge states. This leads to a difference in formation energies of 1.40 eV at the CBM and thus a much higher concentration of In_P^{-2} compared to P_{In}^{-1}. The situation is reversed under P-rich conditions where P_{In}^{q} is favoured across the entire band gap.

2. Indium Arsenide

As illustrated in Fig 3b antisites in InAs are predominently charge neutral. Nevertheless, the low energy defect under stoichiometric conditions is As_{In}^{+1} under *p*-doping conditions although it makes a transition to the neutral charge state at only μ_e = 0.10 eV, which is then dominant right up to the CBM. The same is apparent under As-rich conditions. Under In-rich conditions, the situation is reversed although In_{As}^{q} defects are ~0.3 eV lower in energy than As_{In}^{q} across the entire band gap (so possibly both defects will be observable).

3. Indium Antimonide

Similarly to InAs, the small band gap of InSb negates the formation of many charged defects. Again, we see only the neutral and -1 charge states for In_{Sb}^{q} and the +1 and neutral

charge states for Sb_{In}^{q} . The two transitions predicted from these calculations are $c(0/-)$ = 0.11 eV and $c(+1/0)$ = 0.09 eV for In_{Sb}^{q} and Sb_{In}^{q} respectively.

Stoichiometric conditions favour the formation of Sb_{In}^{q} from the VBM to the CBM, as shown in Fig 3c. The difference in formation energies between the two antisites is, however, not large and as such both defects should be observed. While Sb_{In}^{q} remains more stable than In_{Sb}^{q} under Sb-rich conditions, the difference between formation energies is now much greater so that only Sb_{In}^{q} defects should be observed. Changing the growth conditions to In-rich switches the preference to In_{Sb}^{q}, which is now strongly favoured over Sb_{In}^{q}.

IV. TRENDS

The transition levels for all defects considered above are summarised in Table I. It is noticeable that only the phosphide antisites (P_{Al}^{q} , P_{Ga}^{q} and P_{In}^{q}) possess a stable +2 charge state in which the transition to +1 occurs at Fermi levels that decrease down the group. Interestingly, with the exception of Ga_{As}^{-3} none of the antisites favour the 3+ charge state.

In general, group III antisites dominate under III-rich conditions while group V antisites are dominant under V-rich conditions. There are a few exceptions when, under certain growth conditions, the two antisites exhibit similar formation energies. This is the case for AlSb for which under stoichiometric conditions, Sb_{Al}^{q} dominates in the first half of the band gap and Al_{Sb}^{q} in the second. Under Al-rich conditions, the formation energy of Sb_{Al}^{q} is low enough for it to form under *p*-doping conditions before Al_{Sb}^{q} becomes lower in energy. Likewise, under Sb-rich conditions towards *n*-doping conditions Al_{Sb}^{q} becomes more favourable. This behaviour, by which the group III antisite becomes favourable under group V-rich conditions under *n*-doping conditions, is shared by GaP and GaAs. Overall, group V antisites are most likely to form under stoichiometric conditions. The only compound to favour group III antisites for the entire band gap under stoichiometric conditions is GaSb.

The formation energies of antisites under stoichiometric conditions for Fermi levels in the middle of band gaps (i.e. intrinsic doping conditions) are shown in Table II. This demonstrates a trend similar to the one established previously[16] for vacancies in III-V semiconductors. That is, V_{III}^{q} show a consistent decrease in formation energies with increase in group III or group V covalent radii, while formation energies of III_{V}^{q} decrease with increasing covalent radius of group V atoms; the Ga_{V}^{q} defect is always lower in energy than the corresponding Al_{V}^{q} or In_{V}^{q} defects.

Table II also shows that under stoichiometric growth and doping conditions III_{V}^{q} exists in -1 or -2 charge states. Ga-V compounds favour the -2 charge state while In-V compounds will favour -1 charge state. The other remarkable feature is the prevalence of the neutral charge for all group V antisites. Furthermore, Table II indicates that under intrinsic conditions:

(a) The lowest energy antisites for Al-V are the group V antisites (P_{Al}^{0} , As_{Al}^{0} and Sb_{Al}^{0}).

(b) The lowest energy antisites for Ga-V are the group III antisites (Ga_{P}^{-2} , Ga_{As}^{-2} and Ga_{Sb}^{-2}).

(c) The lowest energy antisites for In-V are the group V antisites (P_{In}^{0} , As_{In}^{0} and Sb_{In}^{0}).

To appreciate the importance of antisites in III-V semiconductors, it is useful to compare their formation energies with those of the vacancies obtained from previous work using the same methodology.[16] Using Table I from Ref. 16 and Table II here we find that the lowest energy antisite is lower in energy than the corresponding lowest energy vacancy defect for all of these III-Vs. The largest difference between antisite and vacancy formation energies occurs in AlP where the difference is $E^{f}\,(V_{P}^{+1}) - E^{f}\,(P_{Al}^{0})$ = 0.85 eV and the least difference occurs in AlSb where $E^{f}\,(V_{Al}^{-2}) - E^{f}\,(Sb_{Al}^{0})$ = 0.09 eV. The differences are summarised in Table III. These can be used to deduce the ratio of antisite to vacancy concentrations by using the relation:

$$c \;=\; N\,exp(-E^{f}/kT\,) \qquad (3)$$

where, c is the concentration, N is the number of sites available, k the Boltzmann's constant and T the temperature. The ratio of antisite concentrations c_A to vacancies concentrations c_V can

then be expressed as:

$$\frac{C_A}{C_V} = \exp(\Delta E^f / kT) \quad (4)$$

where ΔE^f is the difference in formation energies between the favourable vacancies and antisites for each compound, as given in Table III. This indicates that concentrations of antisites can be orders of magnitudes higher than those of vacancies under strict intrinsic conditions. However, vacancies in many III-V compounds are stable in the -3 charge state and over a wide range of Fermi levels (except InAs and InSb). This leads to rapid changes in formation energies, which alters the relative concentrations of vacancies and antisites. For instance, under stoichiometric and group V rich conditions, group III vacancies in AlP, AlAs, AlSb, GaP and GaAs are favoured within the n-doping regime over antisite defects.

V. CONCLUSIONS

The formation energies of antisites in III-V semiconductors were predicted using density functional theory in order to identify their most stable charge states, as a function of the Fermi level, and under stoichiometric, III and V rich conditions. The charged defect interactions were corrected using the scheme of Freysoldt *et al.*[20, 21]

The antisite formation energies of III_V^q decrease with increasing covalent radius of group V atoms, whereas the formation energies of V_{III}^q decrease with increasing group III or group V covalent radii. III_V^q are dominant under III-rich conditions and V_{III}^q under V-rich conditions. Apart from GaSb all other III-V semiconductors favour the formation of V_{III}^q under stoichiometric conditions.

An understanding of the relative behaviour of point defects under different growth or doping conditions is important to guide the fabrication of efficient devices. The present systematic study of antisite defects in the most technologically important III-V semiconductors is part of a concerted effort to characterize the defect processes of these materials. Alongside recent

work on vacancies in III-V semiconductors[16], it aims to provide a roadmap for future work. Comparison with lowest vacancy formation energies reveals that antisite defect concentrations always dominate over vacancies under stoichiometric conditions when the Fermi level is $E_g/2$. However, occasionally under different growth and doping regimes, vacancy energies drop below those for antisites and thus the favoured intrinsic defect type changes.

ACKNOWLEDGMENTS

Funding for this research was provided by a grant from King Abdullah University of Science and Technology (KAUST). Computing resources were provided by KAUST (www.hpc.kaust.edu.sa) and Imperial College London (www3.imperial.ac.uk/ict/services/hpc).

References

[1]"The international technology roadmap for semiconductors," http://www.itrs.net/

[2]J. A. del Alamo, Nature (London) **479**, 317 (2011).

[3]L. Lin and J. Robertson, Appl. Phys. Lett. **98**, 082903 (2011).

[4]H. P. Komsa and A. Pasquarello, J. Phys.: Condens. Matter **24**, 045801 (2012).

[5]J. L. Roehl, A. Kolagatla, V. K. K. Gangur, S. V. Khare, and R. J. Phaneuf, Phys. Rev. B **82**, 165335 (2010).

[6]S. T. Murphy, A. Chroneos, C. Jiang, U. Schwingenschlögl, and R. W. Grimes, Phys. Rev. B **82**, 073201 (2010).

[7]J. L. Rohl, S. Aravelli, S. V. Khare, and R. J. Phaneuf, Surf. Sci. **606**, 1303 (2012).

[8]S. Adachi, Physical properties of III-V Semiconductor Compounds (Wiley, 1992).

[9]H. Bracht, S. P. Nicols, W. Walukiewicz, J. P. Silveira, F. Briones, and E. E. Haller, Nature (London) **408**, 69 (2000).

[10]H. Bracht, S. P. Nicols, E. E. Haller, J. P. Silveira, and F. Briones, J. Appl. Phys. **89**, 5393 (2001).

[11]H. Bracht and S. Brotzmann, Phys. Rev. B **71**, 115216 (2005).

[12]H. A. Tahini, A. Chroneos, H. Bracht, S. T. Murphy, R. W. Grimes, and U. Schwingenschlögl, Appl. Phys. Lett. **103**, 142107 (2013).

[13]G. Kresse and J. Furthmüller, Phys. Rev. B **54**, 11169 (1996).

[14]J. P. Perdew, K. Burke, and M. Ernzerhof, Phys. Rev. Lett. **77**, 3865 (1996).

[15]E. Blöchl, Phys. Rev. B **50**, 17953 (1994).

[16]H. A. Tahini, A. Chroneos, S. T. Murphy, U. Schwingenschlögl, and R. W. Grimes, J. Appl. Phys. **114**, 063517 (2013).

[17]H. J. Monkhorst and J. D. Pack, Phys. Rev. B **13**, 5188 (1976).

[18]S. B. Zhang and J. E. Northrup, Phys. Rev. Lett. **67**, 2339 (1991).

[19]F. El-Mellouhi and N. Mousseau, Phys. Rev. B **71**, 125207 (2005).

[20]C. Freysoldt, J. Neugebauer, and C. G. Van de Walle, Phys. Rev. Lett. **102**, 16402 (2009).

[21]C. Freysoldt, J. Neugebauer, and C. G. Van de Walle, Phys. Status Solidi B **248**, 1067 (2011).

[22]S. Pöykkö, M. J. Puska, and R. M. Nieminen, Phys. Rev. B **53**, 3813 (1996).

[23]J. E. Northrup and S. B. Zhang, Phys. Rev. B **50**, 4962 (1994).

[24]P. A. Schultz and O. A. von Lilienfeld, Modell. Simul. Mater. Sci. Eng. **17**, 84007 (2009).

[25]M. Hakala, M. Puska, and R. Nieminen, J. Appl. Phys. **91**, 4988 (2002).

[26]C. W. M. Castleton and S. Mirbt, Phys. Rev. B **70**, 195202 (2004).

[27]R. Mishra, O. Restrepo, A. Kumar, and W. Windl, J. Mater. Sci. **47**, 7482 (2012).

TABLE I. The transition levels (in eV above the VBM) of group III and group V antisites.

System	Defect	Thermodynamic Transition				
		(+2/+ 1)	(+1/0)	(0/−)	(−/=)	(=/≡)
AlP	Al_P	···	0.59	1.11	1.66	···
	P_{Al}	0.61	0.99	1.95	2.12	···
AlAs	Al_{As}	···	0.19	0.70	1.68	
	As_{Al}	···	0.46	1.85	···	
AlSb	Al_{Sb}	···	···	0.25	0.67	···
	Sb_{Al}	···	0.41	1.37	···	···
GaP	Ga_P	···	0.07	0.43	1.00	···
	P_{Ga}	0.48	0.58	1.84	2.25	···
GaAs	Ga_{As}	···	···	0.26	0.61	1.33
	As_{Ga}	···	0.19	1.08	1.39	···
GaSb	Ga_{Sb}	···	···	0.04	0.27	···
	Sb_{Ga}	···	0.13	0.47	···	···
InP	In_P	···	0.20	0.68	1.13	···
	P_{In}	0.11	0.50	1.28	···	···
InAs	In_{As}	···	···	0.35	···	···
	As_{In}	···	0.10	···	···	···
InSb	In_{Sb}	···	···	0.11	···	···
	Sb_{In}	···	0.08	···	···	···

TABLE II. The formation energies of the group III and group V antisites (in eV) for $\mu_e = E_g/2$ under stoichiometric conditions. The values in parenthesis correspond to the charge of the vacancy under intrinsic conditions.

	III_V^q		
	P	As	Sb
Al	4.33 (-1)	3.39 (-1)	1.82 (-2)
Ga	1.93 (-2)	1.57 (-2)	0.60 (-2)
In	2.64 (-1)	2.19 (-1)	1.46 (-1)
	V_{III}^q		
	P	As	Sb
Al	3.01 (0)	2.24 (0)	1.65 (0)
Ga	2.70 (0)	1.95 (0)	1.59 (0)
In	2.20 (0)	1.55 (0)	1.29 (0)

TABLE III. The difference in formation energies E^f (vacancy) $-$ E^f (antisite) $= \Delta E^f$ (in eV) between the favourable vacancies and antisites for each of the III-V compounds for $\mu_e = E_g/2$ under stoichiometric conditions.

	ΔE^f		
	P	As	Sb
Al	0.85	0.76	0.09
Ga	0.77	0.25	0.63
In	0.31	0.66	0.36

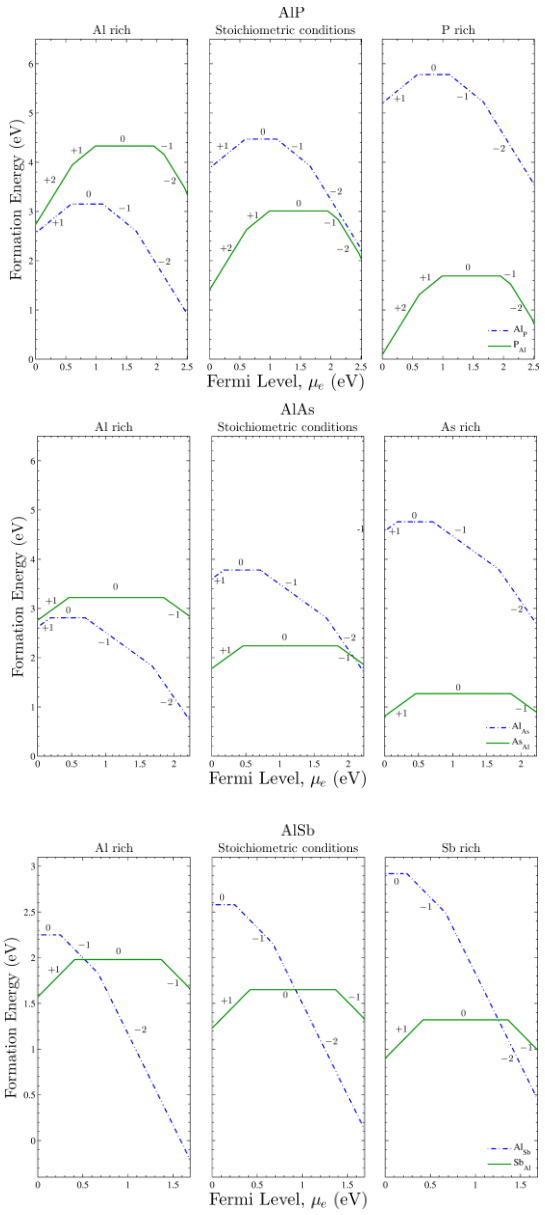

FIG. 1. Lowest energy antisite formation energies for Al-V compounds assuming the most stable charge state (neutral or charged) as a function of the Fermi level. Dashed lines represent the group III antisite and solid lines the group V antisite.

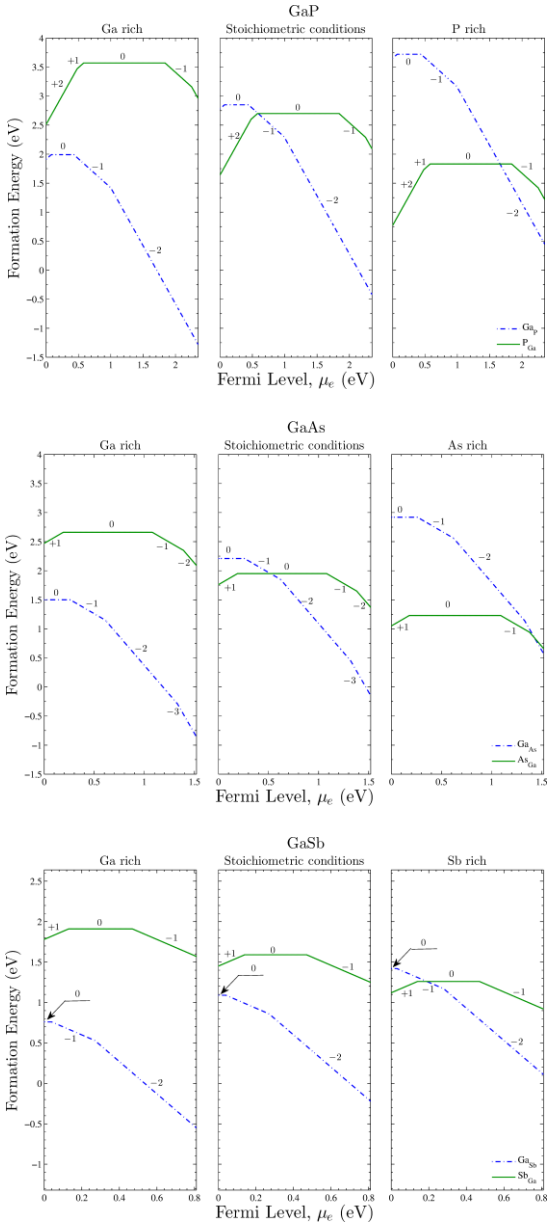

FIG. 2. Lowest energy antisite formation energies for Ga-V compounds assuming the most stable charge state (neutral or charged) as a function of the Fermi level. Dashed lines represent the group III antisite and solid lines the group V antisite.

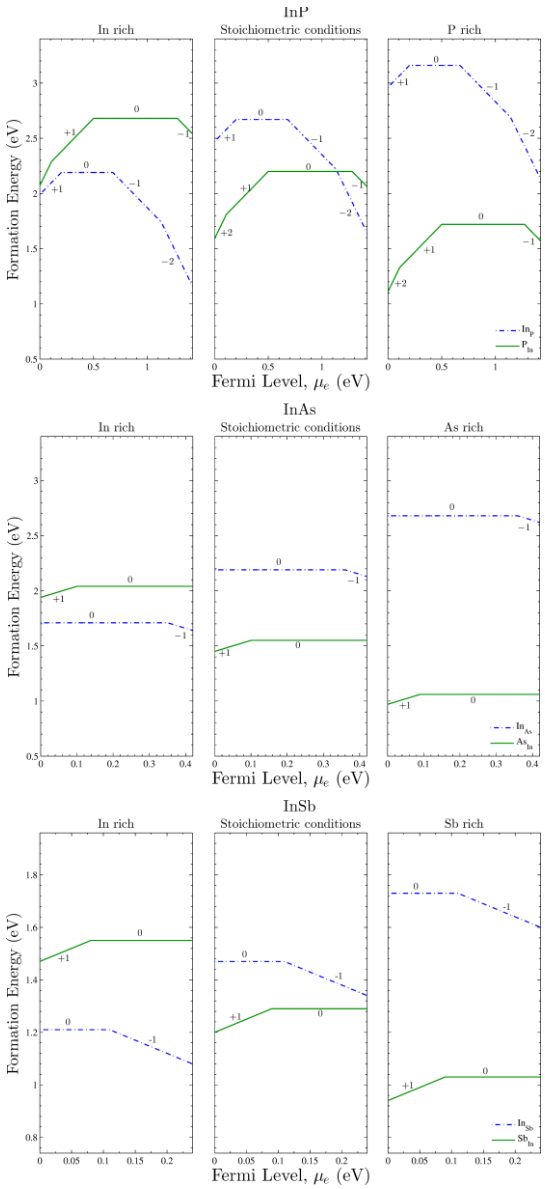

FIG. 3. Lowest energy antisite formation energies for In-V compounds assuming the most stable charge state (neutral or charged) as a function of the Fermi level. Dashed lines represent the group III antisite and solid lines the group V antisite.